

Liveness Detection for Fingerprint Scanners Based on the Statistics of Wavelet Signal Processing

Bozhao Tan and Stephanie Schuckers

Department of Electrical and Computer Engineering, Clarkson University, Potsdam, NY 13699

Abstract

Fingerprint scanners can be spoofed by artificial fingers using moldable plastic, clay, Play-Doh, gelatin, silicone rubber materials, etc. Liveness detection is an anti-spoofing method which can detect physiological signs of life from fingerprints to ensure only live fingers can be captured for enrollment or authentication. In this paper, a new method based on the wavelet transform on the ridge signal extracted along the ridge mask is proposed which can detect the perspiration phenomenon using only a single image. Statistical features are extracted for multiresolution scales to discriminate between live and non-live fingers. Based on these features, we use a classification tree to generate the decision rules for the liveness classification. We test this method on the dataset which contains about 58 live, 80 spoof (50 made from Play-Doh and 30 made from gelatin), and 25 cadaver subjects for 3 different scanners. Also, we test this method on a second dataset which contains 33 live and 33 spoof (made from gelatin) subjects. The proposed liveness detection method is purely software based and application of this method can provide anti-spoofing protection for fingerprint scanners.

1. Introduction

Biometric systems are emerging technologies that enable the authentication of an individual based on physiological or behavioral characteristics, which including recognizing faces, fingerprints, irises, hand geometry, palms, voices, gait and handwriting signatures, etc [1]. Among these biometric identifiers, fingerprint recognition is considered as the most popular and efficient technique. However, the security of fingerprint scanners has been questioned. Previous studies have shown it is possible to fool a variety of fingerprint scanners using a well-duplicated synthetic finger made of silicone rubber, Play-Doh, wax, clay, gelatin, or in the worst cased, dismembered fingers [2, 3, 4]. These materials are moisture based and most fingerprint scanners are able to image them. From a security and accountability perspective, there is an urgent need that a

biometric system should have the capability to detect spoof biometric samples. Liveness detection is an anti-spoofing method ensuring that only “real” fingerprints are capable of generating templates for enrollment, verification and identification [5].

Liveness detection can be performed at the acquisition stage or at the processing stage. Several different techniques have been suggested for liveness detection, such as measuring temperature, pulse, pulse oximetry, blood pressure, electric resistance, or ECG [7, 8, 9, 10]. The main disadvantage of these methods is that they require extra hardware, which is expensive, bulky and not convenient to the users. Another example of liveness detection technique is detecting skin deformation which uses information about how the fingertip’s skin deforms when pressed against the scanner surface [11]. This method considers non-linear distortions between two fingerprint impressions when the user interacts with the sensor service. A thick artificial fingerprint will only give a rigid transformation between two fingerprint images. However, using a thin artificial fingerprint glued on a live finger may still generate a similar non-linear deformation as a live finger would [6].

2. Previous Work

In the previous research, our laboratory has demonstrated that the time-varying perspiration pattern in the fingerprint images can be used as a software based measure to detect liveness. Unlike spoof and cadaver fingers, live fingers have a distinctive spatial phenomenon both statically and dynamically [12]. Based on this principle, a ridge signal algorithm, a wavelet algorithm and an intensity based algorithm have been developed to detect the time-series perspiration pattern for liveness detection.

First, a ridge signal algorithm was developed which maps a 2-D fingerprint image into 1-D “signal” which represents the gray level values along the ridges. Variations in gray levels (between 0 and 2nd or 5th images) correspond to variations in moisture both statically and dynamically. This algorithm extracts one static and 6 dynamic measures and perform liveness classification using back-propagation neural network (BPNN). More

200 details about this algorithm can be referenced in [12, 14].

201 Secondly, a wavelet based approach was developed
202 which concentrated on the changing coefficients using the
203 zoom-in property of wavelet. Multiresolution analysis and
204 wavelet packet analysis are used to extract information
205 from low and high frequency content of the time-series
206 images, respectively. The energy content of changing
207 coefficients is used as a quantified measure to perform the
208 liveness classification [13].

209 Thirdly, an intensity based approach quantified the gray
210 level difference between time-series images using
211 histogram distribution statistics and extracted static and
212 dynamic features which can quantify distinct differences
213 between live and non-live fingerprint images. Based on
214 these static and dynamic features, the decision rules are
215 generated using a classification tree method [15, 16].

216 These methods extract some excellent features using
217 different algorithmic approaches and are capable of
218 producing classification rates in the range of 84%~100%
219 for the three scanners tested. However, all methods require
220 time-series images, which may be convenient for users.
221 Because the perspiration pattern is demonstrated not only
222 dynamically but also statically in our experiments, we
223 consider if it is possible to detect the perspiration
224 phenomenon from a single image only. Detection of
225 perspiration pattern in one image for liveness detection
226 with reasonable performance is the motivation for this
227 work. In this paper, a new method is proposed to quantify
228 the perspiration pattern which applies wavelet
229 decomposition on the ridge signal extracted from a single
230 fingerprint image.

231 3. Data Collection

232 Three types of fingerprint scanners were used to collect
233 data in our study: capacitive DC (Precise Biometrics,
234 100sc), optical (Secugen, EyeD hamster model
235 #HFDUO1A) and electro-optical (Ethentica, USB2500).
236 These systems were selected based on considerations of
237 technology diversity, availability and flexibility of the
238 SDK, and the ability to collect a time series of raw images.
239 For each device, fingerprints images were collected from
240 live, spoof and cadaver fingers. The dataset contains
241 approximately 58 live (from different races, ages and
242 balanced number of males and females), 80 spoof (50 made
243 from Play-Doh and 30 made from gelatin) and 25 cadaver
244 fingerprints.

245 Also we tested our proposed on the dataset collected by
246 Michigan State University called MSU Gummy Finger
247 Database (Ver.1). The dataset is collected from 33 live
248 fingers and corresponding gummy fingers, each of which
249 has 10 impressions with rotation and varying pressures. It is
captured by Identix DFR 200 which is an optical scanner
with 380dpi.

250 Table 1 summarizes the number of subjects used for each
251 device and category. The spoof and cadaver fingerprints
252 are included in the “non-live” category. The image utilized
253 in this paper is the first image immediately after placement
254 on the scanner in time-series collection.

Category	Precise	Secugen	Ethentica	Identix
Live	58	58	55	33
Spoof	80	80	80	33
Cadaver	33	25	22	

255 Table 1. Number of subjects used for each device and category

260 4. Algorithm

261 Figure 1 shows a typical example of the first image
262 captured from live, Play-Doh, gelatin and cadaver fingers
263 in the time-series collection, respectively. As can be
264 observed, compared to the spoof and cadaver fingerprint,
265 live fingerprint has a distinctive gray level difference
266 because the presence of perspiration. In live fingers,
267 perspiration starts from the pores, either completely
268 covering them which makes them wet or leaving the pores
269 as a dry dot. Typically the live fingerprint looks patchy
270 compared to spoof and cadaver fingerprints due to this
271 special phenomenon specific to live fingers [12]. Here we
272 should note that the fingerprint images in our database are
273 the 0 second images immediately after the placement of the
274 fingers. For the live fingers, the perspiration has not
275 diffused along or among the ridges except for very wet
276 fingers, which makes the live fingers look patchy. The
277 basis of this method is simple and straightforward. The
278 gray level along the ridges in live fingers has a distinctive
279 difference and changes with a specific frequency pattern
280 due to the presence of perspiration and pores, compared to
281 the spoof and cadaver fingers.

282 Based on this principle and our previous work, a new
283 method is developed to quantify this phenomenon in a
284 single image. The underlying process is to extract the ridge
285 signal which represents the gray level values along the
286 ridge mask and use wavelet transform to decompose this
287 signal into multi-scales. Static features are extracted on
288 each scale which can quantify the perspiration pattern to
289 discriminate between live and non-live fingerprints. The
290 main steps of this algorithm include:

- 291 1. Fingerprint enhancement;
- 292 2. Ridge mask and signal extraction;
- 293 3. Wavelet decomposition;
- 294 4. Statistical feature extraction;
- 295 5. Classification.



Figure 1: Example of live and non-live fingerprints captured by Capacitive DC scanner: (a) live finger; (b) spoof finger made from Play-Doh; (c) spoof finger made from gelatin; (d) cadaver finger

4.1. Fingerprint Enhancement

To improve the clarity of ridge and valley structures in fingerprint images, a number of techniques have been proposed to enhance gray-level images because the ridge and valley structures in a local neighborhood form a sinusoidal-shaped wave with well-defined frequency and orientation [18, 20]. Here, we use the enhancement algorithm proposed in Hong et al. [18], which applied a bank of bandpass Gabor filters on the normalized fingerprint image using estimated orientation and frequency information.

4.1.1 Pre-processing

The captured fingerprint image may not be clean because of latent fingerprint impressions deposited on the scanner surface. A simple median filter is used to remove this kind of sand and pepper type of noise. Second, to segment the foreground region of interest, the whole image is divided into blocks of small size and the variance of each block is computed. If the variance of a block is less than a threshold value, then it is removed from original image.

4.1.2 Local orientation estimation

The fingerprint has a consistent structure of ridges and valleys in a local neighborhood. The local ridge orientation is commonly used to tune the filter parameters for enhancement. In the Hong et al. enhancement algorithm, a

least mean square orientation estimation method is used. The local orientation in an image can be computed by

$$v_x(i, j) = \sum_{u=i-w/2}^{i+w/2} \sum_{v=j-w/2}^{j+w/2} 2\sigma_x(u, v)\sigma_y(u, v) \quad (1)$$

$$v_y(i, j) = \sum_{u=i-w/2}^{i+w/2} \sum_{v=j-w/2}^{j+w/2} (\sigma_x^2(u, v) - \sigma_y^2(u, v)) \quad (2)$$

$$\theta(i, j) = \frac{1}{2} \tan^{-1} \left(\frac{v_y(i, j)}{v_x(i, j)} \right) \quad (3)$$

where $\theta(i, j)$ is the least square estimate of the local ridge orientation at the block centered at pixel (i, j) . σ_x and σ_y represent the horizontal and vertical gradients. w is the window width for the block wise calculation. Here this method is processed at a block size of 16×16 .

4.1.3 Local frequency estimation

The local ridge frequency is another important property in a fingerprint image. To get the local ridge frequency, X-signatures of each block are computed along the direction perpendicular to the orientation angle in each block. The window used for this purpose is of size 16×32 . The frequency is then computed by the distance between the peaks obtained in the X-signatures. The X-signature for this is given by the formula

$$X[k] = \frac{1}{w} \sum_{d=0}^{w-1} I(u, v), k = 0, 1, \dots, l-1 \quad (4)$$

$$u = i + (d - \frac{w}{2}) \cos O(i, j) + (k - \frac{l}{2}) \sin O(i, j) \quad (5)$$

$$v = j + (d - \frac{w}{2}) \sin O(i, j) + (\frac{l}{2} - k) \cos O(i, j) \quad (6)$$

where I is the input image and O is the orientation image.

Based on experiments, we find that a median frequency of all blocks can be used to represent the whole frequency image for further Gabor filter processing.

4.1.4 Filtering using Gabor filter

Gabor filters consider both the frequency components as well as the spatial coordinates, which make it an excellent non-linear tool in spatial and frequency domains. After getting local orientation angle and frequency, a bank of Gabor filters is applied as a band-pass filter which removes the noise and enhances the ridge and valley structures. The even-symmetric Gabor filter has the general form.

$$h(x, y; \phi, f) = \exp \left\{ -\frac{1}{2} \left[\frac{(x \cos \phi)^2}{\delta_x^2} + \frac{(y \sin \phi)^2}{\delta_y^2} \right] \right\} \cos(2\pi f x \cos \phi) \quad (7)$$

where ϕ is the orientation, f is the frequency, δ_x and δ_y are the parameters of Gaussian function along x and y axis.

To estimate the local orientation and frequency block wise, we need to take into consideration corrupted ridge and valley structures and the existence of minutiae in the

fingerprint images. In these kinds of situations, we can use low pass filtering and interpolation techniques to reduce its negative effects. For the details about this algorithm, we can refer to [18]. Figure 2 shows the outcome of performing orientation estimation, frequency estimation and Gabor filtering.

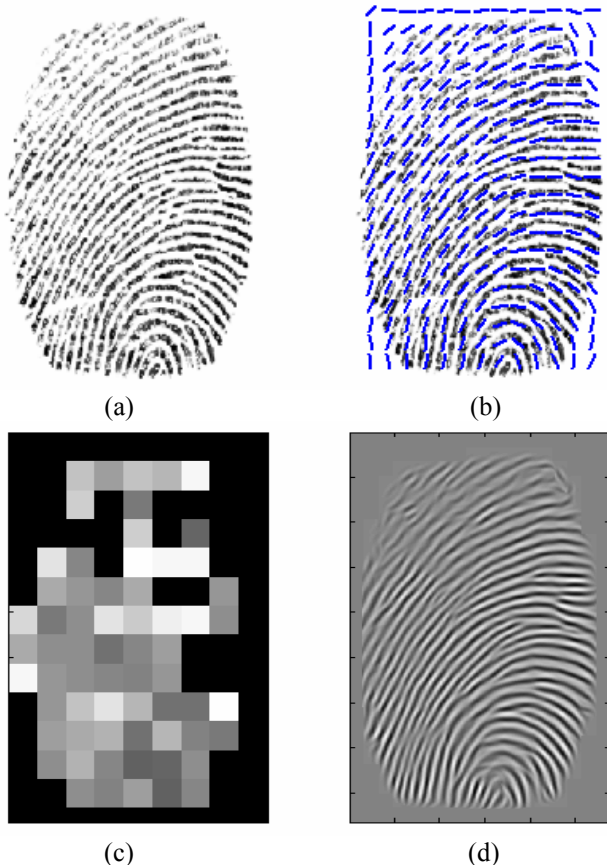


Figure 2: The process of fingerprint enhancement: (a) original image; (b) orientation estimation; (c) frequency estimation; (d) enhanced by Gabor filter

4.2. Ridge mask and signal extraction

After the input fingerprint image is enhanced with Gabor filtering, a binary image is extracted by comparison with a pre-defined threshold. A standard thinning algorithm using morphological operations can be used to obtain one pixel thin ridges. Y-junctions and some short curves shorter than a typical pore-to-pore distance are discarded using a simple non-overlapping neighbor operation. Then the final contour along the ridges can be used as a mask to generate signals corresponding to the actual gray level changes along the ridges. Figure 3 shows the binary output image, the extracted mask superimposed on the original fingerprint and the extracted ridge signal.

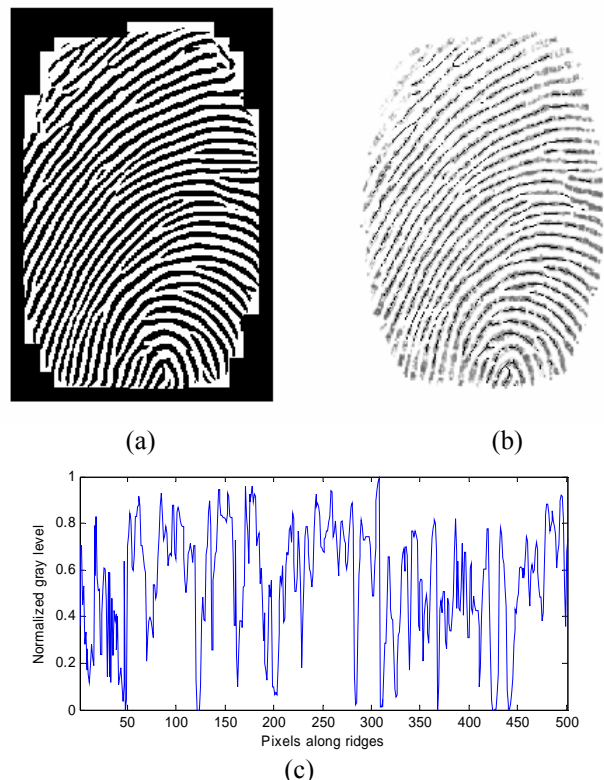


Figure 3: Ridge signal extraction: (a) binary image; (b) thinned ridges laid on the original image; (c) enlarged ridge signal

4.3. Wavelet decomposition

As observed from the extracted ridge signal, it is a non-stationary signal. The Fourier Transform (FT) would not be effective, because FT may not provide appropriate information when analyzing non-stationary signals. Although short time Fourier Transform (STFT) can map the signal into time and frequency domain, it may not be effective because it only uses a fixed window technique. Compared to FT and STFT, the wavelet transform, provides a powerful tool for non-stationary signal processing. From an algorithmic point of view, the 1-D multiresolution analysis leads to dyadic pyramidal implementations using filter banks [19].

The procedure of multiresolution decomposition of a signal is schematically shown in Fig. 4. Each stage of this analysis consists of a highpass and lowpass filter followed by scale two downsampling. In this scheme, the scaling function and mother wavelet function can be calculated by:

$$\phi(n) = 2 \sum_n h_n \phi(2x - n) \quad (8)$$

$$\psi(n) = 2 \sum_n g_n \phi(2x - n) \quad (9)$$

where h_n and g_n are conjugate mirror filters. The output of the first high-pass and low-pass filters provide the detail

D1 and the approximation A1, respectively. The first approximation, A1 is then decomposed to the second level detail D2 and approximation A2, and so on.

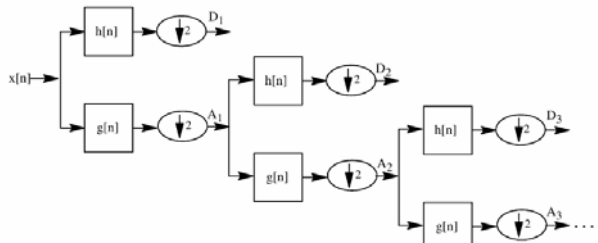


Figure 4: The wavelet multiresolution decomposition scheme

Selection of the mother wavelet is very important when applying the wavelet transform. Usually tests are performed with different types of wavelets and the one which gives maximum efficiency is selected for a specific application. Based on our experiments, Daubechies wavelet is selected as the smoother mother wavelet because it can extract efficient information from different scales. The following figure is the constructed Daubechies scale function and wavelet function. In this method, the level selected is 5 because the further decomposition detail does not contain much useful frequency content.

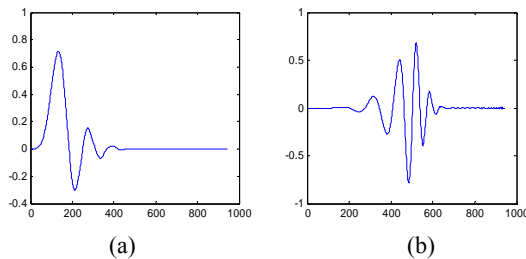


Figure 5: (a) Daubechies scale function (b) wavelet function

Figures 6, 7 and 8 show examples of decomposed wavelet transform on the ridge signal from a typical live, spoof (Play-Doh), and cadaver finger. As can be observed from the comparison, live fingerprints have a higher amplitude and periodic change on some detail scales than those from the spoof and cadaver fingerprints.

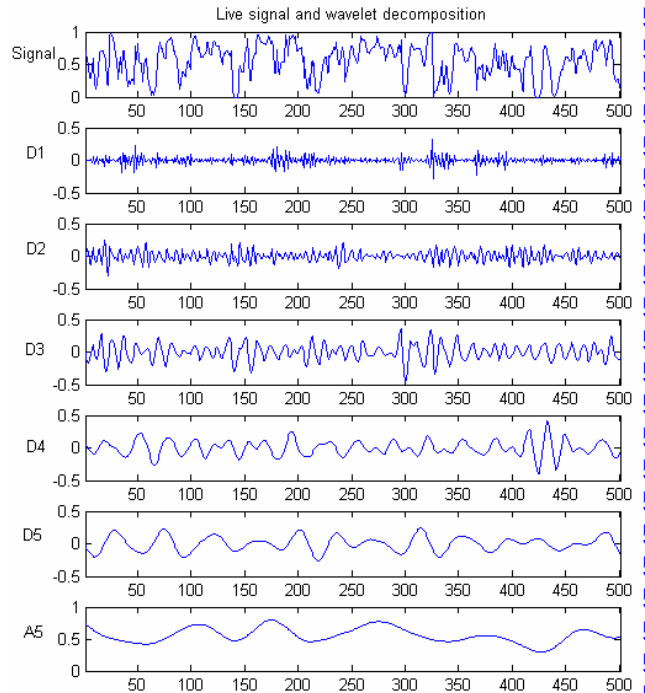


Figure 6: Live signal and wavelet decomposition example

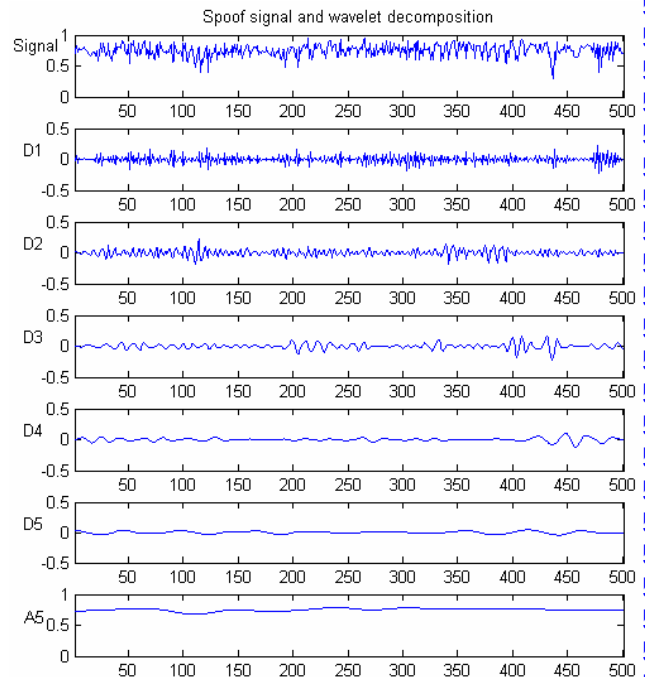


Figure 7: Spoof signal and wavelet decomposition example

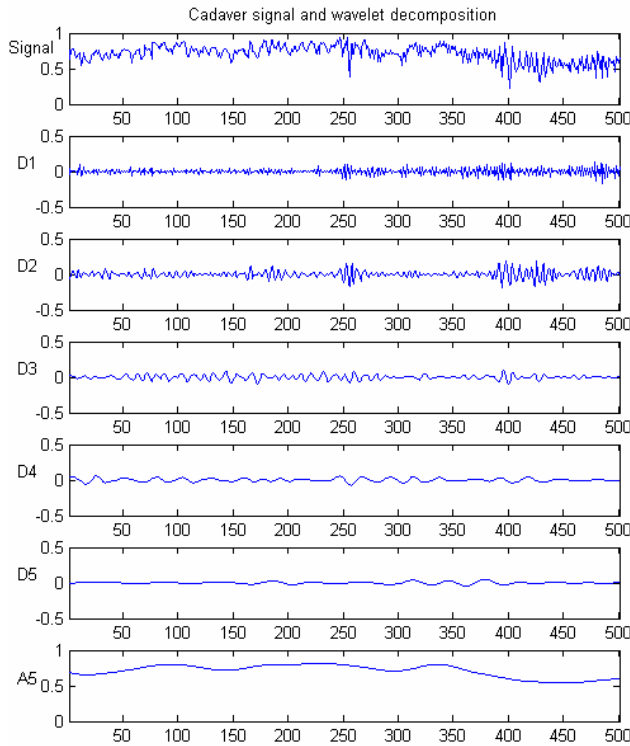


Figure 8: Cadaver signal and wavelet decomposition example

4.4. Statistical feature extraction

The transformed wavelet coefficients provide a compact representation that shows the energy distribution of the signal both in time and frequency. To extract the feature vectors, mean and standard deviation of the wavelet coefficients in each subband are used. Besides the two parameters, mean and standard deviation, from the original signal, we extract 14 parameters including 10 from the 5 detail subbands (D1~D5) and 2 from the last approximation A5. After investigating each parameter on the training and validation dataset, efficient statistical parameters are retained.

For example, Figures 9 and 10 are the comparison of mean and standard deviation in the 4th detail level D4 between live, spoof and cadaver fingerprints, respectively.

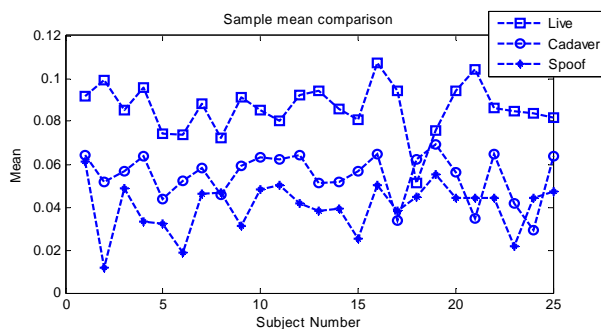


Figure 9: D4 mean comparison in capacitive DC scanner

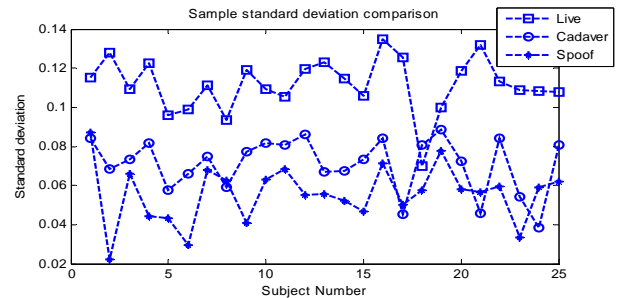


Figure 10: D4 standard deviation comparison in capacitive DC scanner

4.5. Classification

In this algorithm, classification trees are used to separate the non-live subjects from the live subjects. Classification trees derive a sequence of if-then-else rules using the training set in order to assign a class label to the input data. The user can see the decision rules clearly to verify if the rules match their understanding about the classification. In our samples, while there are general trends, there are also some live fingers which may be very wet and change very little along the ridges. In addition, some cadaver images look like live fingers but still have grey level differences in some subbands compared with live fingerprints. The classification tree works efficiently taking into consideration these situations. In our case, an Excel tool developed by Dr. A. Saha was applied to generate the classification tree automatically [17]. The training, validation and test data is randomly selected. Fig. 11 shows the classification tree selected for the capacitive DC scanner. For example, in this decision tree, the enrolled subject is classified as live if the first feature E (mean of detail D4) is larger than 0.068099 and the second feature B (mean of detail D3) is larger than 0.65592, which matches our observation in the former discussion. Support means how many percent of the training data are supported by this rule and confidence means the confidence level about this specific decision rule. Classification of images is divided into live and non-live categories where non-live category includes images from Play-Doh, gelatin and cadavers.

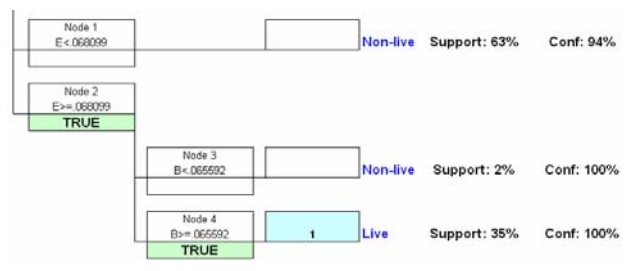


Figure 11: Classification tree for capacitive DC scanner

5. Results and discussion

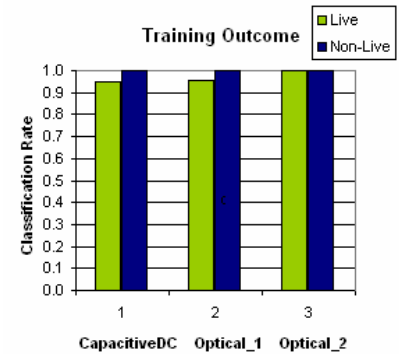
To evaluate this algorithm objectively, the dataset is divided into training (4/9), validation (2/9) and test (1/3) datasets. The randomly selected training and validation data is used to generate and determine the classification tree. The decision tree which has the least FAR and FRR scores is chosen as the one most likely perform well on the unseen test data.

Fig. 12 presents the training and test results for live and non-live fingerprints based on this new statistics of wavelet decomposition approach. The capacitive DC (Precise) scanner demonstrates between 90-100% (for live and non-live, respectively) correct classification rate. The optical scanner (Secugen) in our dataset demonstrates between 80-92% correct classification rate. The other optical scanner (Identix) has a classification rate between 84.6-93%. However, the electro-optical scanner (Ethentica) does not achieve a good classification when applying this method on one single image only. The reason we think is because the capacitive DC and optical scanners are more sensitive to the characteristics in one image. The electro-optical scanner shows the perspiration pattern across time, as seen in previous work [12~16]. However, single image characteristics are similar for live, spoof and cadaver fingers.

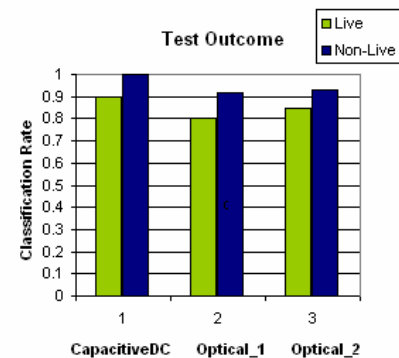
Figure 13 shows some examples where the algorithm fails in the capacitive DC scanner. When the live fingers are very wet and perspiration saturated, there is a little variation along the ridges. In this kind of situation, quickly wiping the clothes is effective in most cases to demonstrate a live pattern. Also sometimes it can be more difficult to classify some cadaver fingers. From the comparison, we find it is much easier to classify spoof (made from Play-Doh and gelatin).

This research demonstrates that the vitality of fingerprints can be determined by a new method processing only a single image. These images were the first image immediately upon placement on the fingerprint scanner. It is not known if this would be applicable to “any” fingerprint image since some devices wait until full development of the image before matching (~1 sec). However, if this algorithm is integrated with a system presumably, the “first” image would be available. The outcome compares with methods using time-series images. Because this method is based on detection of perspiration along the fingerprints, wiping the clothes before scanning may be necessary.

Another issue of this method is that it is device-dependent because the fingerprint images vary across different technologies. Different and efficient features will need to be generated for different scanners when applying this method.



(a) Training outcome



(b) Test outcome

Figure 12: Results on three different scanners



Figure 13: Fail examples: (a) live fingers are classified as non-live fingers; (b) cadaver fingers are classified as live fingers

Further research for this work is to investigate this method on a larger dataset. Our plan is to collect more live subjects to detect the variation of perspiration phenomenon. Also we plan to collect more spoof data using gelatin, Play-Doh and silicone rubber materials to see if we can use these materials to simulate the perspiration phenomenon. Also to improve this method, more analysis of effective features on the multiresolution scales is needed to optimize this method and improve its efficiency.

6. Conclusion

A new method which applies wavelet transform on the ridge signal extracted along the fingerprint images is proposed to detect liveness. Results show that it is possible for the capacitive DC and optical scanners to detect vitality using a single fingerprint based on the perspiration pattern specific to the live fingers. The method is purely software based and application of this liveness detection method can protect fingerprint scanners from spoof attacks.

Acknowledgments

This work is funded by NSF ITR grant #0325333 and Center for Identification Technology Research (CITeR) at West Virginia University. We also thank Dr. Anil K. Jain from Michigan State University for supplying the MSU Gummy Finger Database (Ver.1).

References

- [1] A. Jain, R. Bolle, S. Pankanti, Biometrics: Personal Identification in Networked Society, Springer, 1999
- [2] S. A. C. Schuckers, Spoofing and anti-spoofing measures, Information Security Technical Report, Vol. 7, No. 4, pages 56 – 62, 2002.
- [3] T. Matsumoto, H. Matsumoto, K. Yamada, and S. Hoshino, Impact of artificial ‘gummy’ fingers on fingerprint systems, Proceedings of SPIE, vol. 4677, January, 2002
- [4] H. Kang et. al., A Study on Performance Evaluation of the Liveness Detection for Various Fingerprint Sensor Modules, Lecture notes, Volume 2774, pp 1245-1253, 2003
- [5] Liveness Detection in Biometric Systems, International biometric group white paper, available at <http://www.ibgweb.com/reports/public/reports/liveness.html>
- [6] M. Sandstrom, Liveness Detection in Fingerprint Recognition Systems, Master thesis, <http://www.ep.liu.se/exjobb/isy/2004/3557/exjobb.pdf>
- [7] D. Osten, H. M. Carim, M. R. Arneson, B. L. Blan, “Biometric, personal authentication system”, Minnesota Mining and Manufacturing Company, U.S. Patent #5,719,950, February 17, 1998.
- [8] Kurt Seifried, “Biometrics - What You Need to Know,” Security Portal, 10 January 2001
- [9] P. D. Lapsley, J. A. Less, D. F. Pare, Jr., N. Hoffman, “Anti-fraud biometric sensor that accurately detects blood

- flow”, SmartTouch, LLC, U.S. Patent #5,737,439, April 7, 1998. 850
 - [10] 11. P. Kallo, I. Kiss, A. Podmaniczky, and J. Talosi, “Detector for recognizing the living character of a finger in a fingerprint recognizing apparatus”, Dermo Corporation, Ltd. U.S. Patent #6,175,64, January 16,2001. 851
 - [11] D.Maltoni, D. Maio, A. Jain, and S. Prabhakar, Handbook of Fingerprint Recognition, Springer Verlag, Nu, USA, 2003 852
 - [12] R. Derakhshani, S. A. C. Schuckers, L. Hornak, and L. O’Gorman, Determination of vitality from a non-invasive biomedical measurement for use in fingerprint scanners. Pattern Recognition Journal, Vol. 36, No.2, 2003. 853
 - [13] Schuckers SAC, Abhyankar A, A Wavelet Based Approach to Detecting liveness in Fingerprint Scanners, Proceedings of Biometric Authentication Workshop, ECCV, Prague, May, 2004 854
 - [14] Parthasaradhi S, Derakhshani R, Hornak L, Schuckers SAC, Time-Series Detection of Perspiration as a Liveness Test in Fingerprint Devices, IEEE Transactions on Systems, Man, and Cybernetics, Part C: Applications and Reviews, vol. 35, pp. 335- 343, 2005. 855
 - [15] B. Tan, S. Schuckers, Liveness detection using an intensity based approach in fingerprint scanner, Proceedings of Biometrics Symposium (BSYM2005), Arlington, VA, Sept. 19-21 2005 856
 - [16] B. Tan, S. Schuckers, Comparison of Ridge- and Intensity-based perspiration liveness detection methods in Fingerprint Scanners, SPIE Defense and Security Symposium, Apr. 2006, Orlando, Florida USA 857
 - [17] A. Saha, Classification Tree in Excel, Available at <http://www.geocities.com/adotsaha/CTree/CTreeinExcel.html> 858
 - [18] L. Hong, Y. Wang and A. Jain: Fingerprint image enhancement: Algorithm and Performance Evaluation. IEEE Transactions on Pattern Analysis and Machine Intelligence, Aug. 1998 (Vol. 20, No. 8), pp777–789 859
 - [19] M. B. Ruskaei et. al., Wavelets and Digital Signal Processing in Wavelets and Their Applications (pp. 105-121), 1992 860
 - [20] M. Kawagoe and A. Too. Fingerprint pattern classification. Pattern Recognition, 17(3):295-303,1984 861
- 862
- 863
- 864
- 865
- 866
- 867
- 868
- 869
- 870
- 871
- 872
- 873
- 874
- 875
- 876
- 877
- 878
- 879
- 880
- 881
- 882
- 883
- 884
- 885
- 886
- 887
- 888
- 889
- 890
- 891
- 892
- 893
- 894
- 895
- 896
- 897
- 898
- 899